irradiated on a merry-go-round for 4.2–5 min. The 456-nm line of the 450-W medium-pressure mercury vapor Hanovia lamp was isolated by a $CuCl_2/CaCl_2$ filter solution. The samples were open to the air during irradiation to allow oxygen to diffuse in to replace the oxygen consumed during the reaction. The optical densities of the samples at 440 nm before and after irradiation were measured on a Hitachi 100-80 spectrophotometer. All solutions were shielded from the light as much as possible during preparation and after irradiation. The absorbance of rubrene was adjusted to be approximately 1.82–1.86 at the beginning of the experiment. The furan concentrations were adjusted so that about 25% of the rubrene was consumed. While 50% of the rubrene was consumed in cuvettes with no furan. Reaction rate constants were calculated from

$$k_A = \frac{k_{ox}([R]_f^D - [R]_f^O) + k_d \ln ([R]_f^D/[R]_f^O)}{[D] \ln ([R]/[R]_f^D)}$$

where $k_{ox} = 3.3 \times 10^7$ s^{-1} and is the rate constant for the reaction of singlet oxygen with rubrene in methylene chloride. [R] is the initial rubrene concentration and $[R]_f^D$ and $[R]_f^O$ are the final rubrene concentrations in the presence and absence of diene (furan). [D] is the furan concentration and k_d is the rate of decay of singlet oxygen in methylene chloride (1×10^4 s^{-1}).[74-76]

Two kinetic determinations were made for each compound. Each kinetic run resulted in two rate constants. If there was not good agreement among these four numbers (±10%) an additional kinetic determination was conducted.

Young's Kinetic Technique. The rate of disappearance of diphenylisobenzofuran (DPBF) due to reaction with singlet oxygen is monitored at its emission wavelength of 460 nm. The kinetic scheme for the disappearance of DPBF in the presence of diene substrates is given by

$$\mathrm{DPBF} + {}^1O_2 \xrightarrow{k_f} (\mathrm{DPBF})O_2$$

$$\mathrm{diene} + {}^1O_2 \xrightarrow{k_r} (\mathrm{diene})O_2$$

$$\mathrm{diene} + {}^1O_2 \xrightarrow{k_q} \mathrm{diene} + {}^3O_2$$

$${}^1O_2 \xrightarrow{k_d} {}^3O_2$$

The steady-state treatment for the disappearance of DPBF gives

$$\frac{-d[\mathrm{DPBF}]}{dt} = K\left[\frac{k_f[\mathrm{DPBF}]}{k_f[\mathrm{DPBF}] + k_r[\mathrm{diene}] + k_q[\mathrm{diene}] + k_d}\right]$$

The fluorescent acceptor (DPBF) is present in extremely low concentrations so that is disappearance is cleanly first order.

$$\frac{-d[\mathrm{DPBF}]}{dt} = K\left[\frac{k_f[\mathrm{DPBF}]}{k_r[\mathrm{diene}] + k_q[\mathrm{diene}] + k_d}\right]$$

Under conditions in which the diene does not appreciably react a plot of log fluorescence vs. time is linear with slope S. A plot of S_O/S_D where

$$S = K\left[\frac{k_f}{k_r[\mathrm{diene}] + k_q[\mathrm{diene}] + k_d}\right]$$

S_O is the slope in the absence and S_D in the presence of diene vs. diene concentration has a slope of $(k_r + k_q)/k_d$.

The Young kinetic studies were carried out with a Perkin-Elmer MPF-2A spectrophotometer. The photolyzing light absorbed by the dye was produced by a Sylvania 750 Q/Cl tungsten–halogen lamp operated at 36–45 vs. This irradiation source was placed at right angles to the excitation (418 nm) and emission (460 nm) light paths and focused through a Corning 3-68 filter (cutoff 540 nm). Eight stock solutions with a variety of diene concentrations were utilized for each determination. At least two determinations were made for each compound, and additional measurements were made if good agreement (±10%) was not obtained.

Acknowledgment. We are grateful to the donors of the Petroleum Research Fund, administered by the American Chemical Society, for support of this research. We also thank Kathleen K. Lewis for assistance in the synthesis of endoperoxides and furans.

Registry No. 5a, 625-86-5; **5b**, 4789-40-6; **5c**, 955-83-9; **5d**, 110-00-9; **5e**, 32460-00-7; **5f**, 4282-32-0; **5g**, 53662-83-2; **5h**, 823-82-5; **5i**, 25414-22-6; **5j**, 7040-43-9; **5k**, 534-22-5; **5l**, 584-12-3; **5m**, 611-13-2; **5n**, 614-99-3; **5o**, 617-90-3; **5p**, 98-01-1; **5q**, 6132-37-2; **5r**, 13714-86-8; **5s**, 620-02-0; **5t**, 17113-31-4; **5u**, 17113-32-5; **5v**, 17113-33-6; **5w**, 14297-34-8; **5x**, 17221-37-3; **5y**, 35461-96-2; **5z**, 64468-77-5; **5aa**, 28123-72-0; **5bb**, 1230-48-4; **5cc**, 57196-75-5; **5dd**, 36710-36-8; **5ee**, 36710-35-7; **6a**, 13693-26-0; **6b**, 89088-41-5; **6c**, 4982-34-7; **6d**, 89088-42-6; **6e**, 58864-06-5; **6f**, 80109-14-4; **6g**, 89088-43-7; **6h**, 80109-11-1; O_2, 7782-44-7.

---

(74) Hurst, J. R.; McDonald, J. D.; Schuster, G. B. *J. Am. Chem. Soc.* **1982**, *104*, 2066.

(75) The σ and σ^+ values were taken from: Stock, L. M.; Brown, H. C. In "Advances in Physical Organic Chemistry"; Vol. 1, Gold, V., Ed.; Academic Press: New York, 1963; p 89. The σ value for –CHO was taken from: March, J. "Advance Organic Chemistry, Reactions Mechanisms, and Structure", 2nd ed.; McGraw-Hill: New York, 1977.

(76) The precipitation of furan **5f** during kinetic runs would be expected to lead to a slower than expected rate constant. Indeed, examination of Figure 2 reveals a negative deviation of the point for **5f** from the Hammett linear regression line.

Oxetane: The First X-ray Analysis of a Nonsubstituted Four-Membered Ring

P. Luger* and J. Buschmann

Contribution from the Institut für Kristallographie, Freie Universität Berlin, D-1000 Berlin 33, West Germany. *Received May 11, 1984*

Abstract: Oxetane (C_3H_6O), melting point 174 K, was crystallized on a four-circle diffractometer equipped with a nitrogen gas stream low temperature device. Its structure has been determined by means of single-crystal X-ray analysis at 90 and 140 K. The crystals are orthorhombic, with space group *Pnam* and unit cell dimensions a = 8.620 (4) Å, b = 6.384 (15) Å, c = 6.038 (13) Å, V = 332.3 Å^3 at 90 K and a = 8.657 (1) Å, b = 6.401 (5) Å, c = 6.010 (5) Å, V = 333.0 Å^3 at 140 K, Z = 4. Three-dimensional diffractometer data were refined by least-squares methods to final R values of 3.8% (90 K data) and 4.1% (140 K data). In the crystal the oxetane four-membered ring has exact C_s symmetry and this ring was found to be nonplanar. The angle of pucker is 10.7 (1)° (90 K data) and 8.7 (2)° (140 K data), respectively. The endocyclic C–O bond length, 1.460 (1) Å at 90 K, is unusually large for a C–O single bond.

From the present knowledge of the stereochemistry of cyclobutane and its heterocyclic analogues it is generally accepted that the cyclobutane ring exists in a puckered form with a puckering angle of approximately 30°, whereas oxetane is planar.[1] The

Table I. Crystallographic Data for Oxetane, C_3H_6O, at 90 and 140 K

property	90 K data	140 K data
lattice constants, Å	$a = 8.620$ (4) $b = 6.384$ (15) $c = 6.038$ (13)	$a = 8.657$ (1) $b = 6.401$ (5) $c = 6.010$ (5)
cell volume, Å^3	332.3	333.0
formula units/cell	4	4
X-ray density, g cm^{-3}	1.154	1.151
space group	orthorhombic *Pnam*	orthorhombic *Pnam*
total no. of reflns ($\theta \leq 30°$)	527	606
unobserved ($I < 2\sigma$)	91	212
linear absorption coeff (cm^{-1}, Mo Kα, $\lambda = 0.71068$ Å)	0.92	0.92
R_w,^{a,b} %	5.1	4.9
a^a	0.6	0.6
b^a	5.0	5.0
R value, %	3.8	4.1

^{a}The function minimized was $\sum w(|F_o| - |F_c|)^2$ with $w = xy$; $x = 1$ for $\sin\theta > a$, $x = \sin\theta/a$ otherwise; $y = 1$ for $|F_o| < b$, $y = b/|F_o|$ otherwise. $^b R_w = [\sum w(|F_o| - |F_c|)^2/\sum wF_o^2]^{1/2}(100\%)$.

structural data of oxetane were obtained from microwave spectra[2-5] and from far-infrared spectroscopic investigations[6-8] which yielded relatively precise bonding data.[1]

In addition to the spectroscopic results, a few X-ray investigations of highly substituted oxetane derivatives[9-11] are known which clearly showed the oxetane ring to be nonplanar in the crystal, having puckering angles of up to 23°. It seemed therefore of special interest to investigate the crystal structure of nonsubstituted oxetane to see whether or not the nonplanarity is caused by substituent influences. Here we report the oxetane crystal structure determined from two separate measurements at temperatures of 90 and 140 K. This work is part of a series of X-ray investigations on the crystalline conformations of small cyclic ethers having previously resulted in the disclosure of the tetrahydrofuran[12] and dioxane[13] structures.

Experimental Section

Commercially available oxetane (99% purity, Merck) was used throughout the investigations. A DTA diagram taken between 293 and 133 K showed no further signal below the melting point (at 174 K), and our X-ray investigations down to 90 K always indicated the same crystal lattice. Therefore it is certain that only one phase exists in this temperature range.

Crystal growth was achieved directly on the diffractometer. A few millimeters of sample fluid were brought into the tip of a glass capillary 0.5 mm in diameter and 0.01 mm in wall thickness, which was sealed off to a length of 24 mm. When the capillary was cooled in the nitrogen gas stream of a low-temperature device, polycrystalline material was obtained usually far below the melting point. A single crystal was then grown by partial melting of the polycrystalline solid substance in the direction against the gas stream with a heating coil and by subsequent very slow electronically controlled reduction of heat output from the coil. For observation of the crystallization process the enlarged picture of the capillary was generated on a television monitor via telescope and video camera.

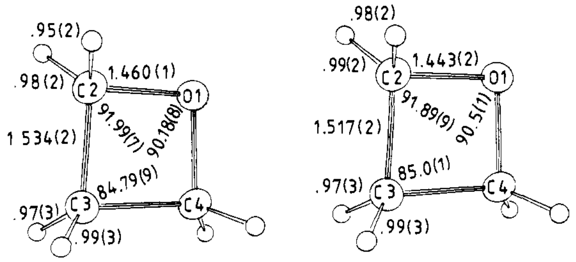

Figure 1. Atom numbering scheme (C4 is the mirror image of C2), bond lengths (Å), and valence angles (deg) for oxetane at the temperatures of 90 K (left) and 140 K (right). Esd's are given in parentheses.

Table II. Final Atomic Parameters (esd's in parentheses) U_{eq}[25] and U in Å^2 × 100

atom	x	y	z	U_{eq} or U
		(a) Oxetane 90 K Data		
C(2)	0.8750 (1)	0.2307 (2)	0.5788 (2)	2.47 (3)
C(3)	0.9322 (2)	0.3904 (2)	0.75 (–)	2.32 (4)
O(1)	0.8440 (1)	0.0747 (2)	0.75 (–)	2.49 (3)
H(21)	0.949 (2)	0.178 (3)	0.476 (3)	3.9 (4)
H(22)	0.778 (2)	0.268 (3)	0.504 (3)	3.6 (4)
H(31)	1.044 (3)	0.409 (4)	0.75 (–)	3.2 (6)
H(32)	0.883 (3)	0.530 (4)	0.75 (–)	3.2 (6)
		(b) Oxetane 140 K Data		
C(2)	0.8756 (2)	0.2305 (2)	0.5795 (2)	3.60 (4)
C(3)	0.9305 (2)	0.3887 (3)	0.75 (–)	3.34 (5)
O(1)	0.8425 (2)	0.0783 (2)	0.75 (–)	3.67 (4)
H(21)	0.952 (2)	0.176 (3)	0.473 (3)	4.8 (5)
H(22)	0.780 (2)	0.269 (3)	0.499 (4)	5.3 (5)
H(31)	1.044 (3)	0.411 (5)	0.75 (–)	5.4 (8)
H(32)	0.877 (3)	0.522 (5)	0.75 (–)	4.7 (7)

Table III. Dihedral Angles (deg) (esd's in parentheses)

sequence	90 K data	140 K data
O(1)-C(2)-C(3)-C(4)	-7.56 (9)	-6.1 (1)
C(4)-O(1)-C(2)-C(3)	7.9 (1)	6.4 (1)
C(2)-O(1)-C(3)-C(4)	168.8 (1)	171.0 (2)
O(1)-C(2)-C(4)-C(3)	169.3 (1)	171.3 (2)
H(31)-C(3)-C(2)-O(1)	106 (1)	108 (1)
H(32)-C(3)-C(2)-O(1)	-126 (1)	-123 (1)
H(31)-C(3)-C(2)-H(21)	-8 (2)	-7 (2)
H(32)-C(3)-C(2)-H(22)	-13 (2)	-10 (2)

The crystal quality was then examined by scans over different reflections and by displaying their profiles on a Tektronix graphic screen. A suitable crystal of oxetane was cooled down to temperatures of 140 and 90 K, where the X-ray measurements were carried out.

At both temperatures oxetane has the orthorhombic space group *Pnam* with four molecules in the unit cell. The relevant crystallographic data are summarized in Table I. Precise lattice constants and the intensity data of an octant (*hkl* all >0) were measured on a DEC PDP 15/40 controlled SIEMENS four-circle diffractometer with Zr-filtered Mo Kα radiation ($\lambda = 0.71068$ Å). The lattice constants were refined from 15 high-order reflections. The intensity data were recorded by using the θ–2θ scan technique.

A variable scan range $\Delta\theta$ was used with $\Delta\theta = 0.80 + 0.47 \tan\theta$. Maximum and minimum scan speeds were 0.33 and 0.02 deg/s. In each background counting rates were measured stationarily for half the time needed for the reflection scan.

For the 90 K data set additional high-order reflections up to $(\sin\theta)/\lambda = 1$ were taken to allow a later evaluation of X–X deformation density maps.

Structure Determination. Phase determination was carried out successfully with direct methods (MULTAN).[14] The refinement with least-

---

(1) Moriarty, R. M. *Top. Stereochem.* **1974**, *8*, 271.

(2) Gwinn, W. D.; Zinn, J.; Fernandez, J. *Bull. Am. Phys. Soc.* **1959**, *4*, 153.

(3) Chan, S. I.; Zinn, J.; Gwinn, W. D. *J. Chem. Phys.* **1960**, *33*, 295.

(4) Chan, S. I.; Zinn, J.; Fernandez, J.; Gwinn, W. D. *J. Chem. Phys.* **1960**, *33*, 1643.

(5) Chan, S. I.; Zinn, J.; Gwinn, W. D. *J. Chem. Phys.* **1961**, *34*, 1319.

(6) Danti, A.; Lafferty, W. J.; Lord, R. C. *J. Chem. Phys.* **1960**, *33*, 294.

(7) Chan, S. I.; Borgers, T. R.; Russel, J. W.; Strauss, H. L.; Gwinn, W. D. *J. Chem. Phys.* **1966**, *44*, 1103.

(8) Ueda, T.; Shimanouchi, T. *J. Chem. Phys.* **1967**, *47*, 5018.

(9) Noordik, J. H.; Cillissen, J. M. *Cryst. Struct. Commun.* **1981**, *10*, 345.

(10) Holan, G.; Kowala, J.; Wunderlich, J. A. *J. Chem. Soc., Chem. Commun.* **1973**, *34*.

(11) Hospital, M.; Leroy, F.; Bats, J. P.; Moulines, J. *Cryst. Struct. Commun.* **1978**, *7*, 309.

(12) Luger, P.; Buschmann, J. *Angew. Chem.* **1983**, *95*, 423; *Angew. Chem., Int. Ed. Engl.* **1983**, *5*, 410.

(13) Buschmann, J.; Luger, P.; Müller, E. ECM 8 1983, Abstract Book, 133.

(14) Main, P.; Woolfson, M.; Germain, G. "MULTAN, A Computer Programme for the Automatic Solution of Crystal Structures"; University of York: York, Great Britain, 1975.

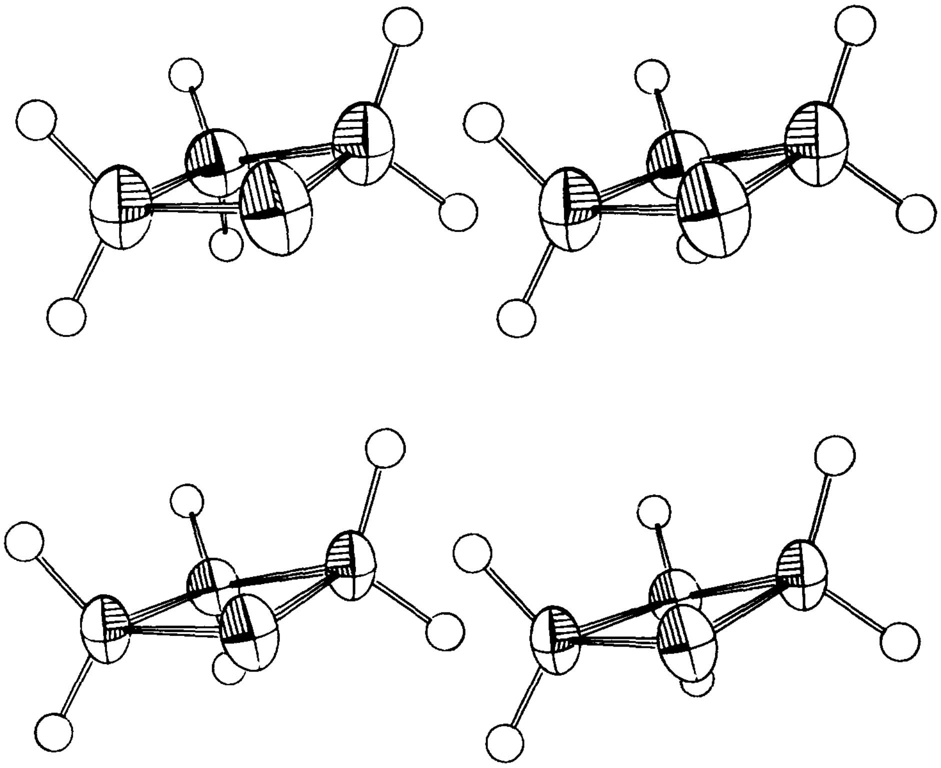

Figure 2. ORTEP[18] stereoviews of the oxetane molecule at 90 K (bottom) and at 140 K (top). The thermal ellipsoids are plotted at a 50% probability level.

Table IV. Bonding Data Obtained for Oxetane and Some Derivatives by Various Methods

		quantity						angle of pucker, deg	ref
compound	method	C-O, Å	C-C, Å	C-H, Å	C—O—C, deg	O—C—C, deg	C—C—C, deg		
oxetane	MW	1.449 (2)	1.549 (3)	1.095 (3)	91.98 (12)	91.73 (5)	84.55 (2)	0	5
	XR (140 K)	1.443 (2)	1.517 (2)	0.98 (3)	90.5 (1)	91.89 (9)	85.0 (1)	8.7 (2)	this work
	XR (90 K)	1.460 (1)	1.534 (2)	0.97 (2)	90.18 (8)	91.99 (7)	84.79 (9)	10.7 (1)	this work
3-oxetanone[a]	MW	1.441 (13)	1.524	1.09[b]	94.82	88.48	88.23 (11)	0	26
3-methyleneoxetane[a]	MW	1.449 (20)	1.523 (20)	1.09[b]			87 (2)	0	27
2-(α-chlorobenzyl)-2-phenyloxetan-2-one[a]	XR (room temp)	1.458 (6)	1.518 (8)		93.9 (3)	88.8 (4)	89.2 (4)	4.7 (6)	9
2-methyloxetane	ED	1.448 (5)	1.534 (4)	1.118 (3)	92[b]	91.2 (15)	85.5 (18)	2.5 (55)	28
3,3-bis(azidomethyl)oxetane	ED	1.458 (7)	1.547 (3)	1.110 (6)	94.0 (16)		87.3 (14)	5.2 (40)	29
2,2-di(*p*-ethoxyphenyl)-3,3-dimethyloxetane	XR (room temp)	1.475						16	10
3,5-dinitrobenzoate of *threo*-3,3,4,4,α-pentamethyl-2-oxetanemethanol	XR (room temp)	1.459	1.554		90.5	90.6	83.6	22.9 (2)	11

[a] Nominal sp^2 hybridization of one carbon atom. [b] Fixed.

squares techniques was executed with the corresponding programs of the X-RAY 76[15] program system. Scattering factors were taken from the standard routine of the X-RAY 76 system.[16,17] An absorption correction was not applied. All hydrogen atoms were located from difference syntheses. During the refinement, which was made with anisotropic temperature factors for the non-hydrogen atoms and isotropic thermal parameters for the hydrogens, a weighting scheme was applied that made $w\Delta F$ independent of $|F|$. This was achieved by setting $w = xy$, with $x = 1$ for $\sin\theta > a$, $x = \sin\theta/a$ otherwise, and $y = 1$ for $F_o < b$, $y = b/F_o$ if $F_o \geq b$ (a and b are given in Table I). Unobserved reflections ($I < 2\sigma(I)$) were included in the refinement only if $|F_c| > |F_o|$. After convergence of all parameters final R values of 3.8% (90 K data) and 4.1% (140 K data) were obtained. The final atomic coordinates are given in Table II. Bond lengths and angles (Figure 1) have standard deviations of 0.001–0.002 Å and 0.07–0.1°.

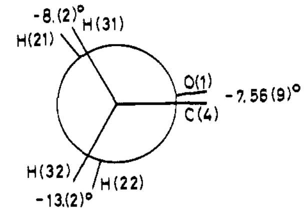

Figure 3. Newman projection down the endocyclic C–C bond C(3)–C(2) illustrating the ring puckering and the nearly eclipsed arrangement of the hydrogen atoms. The numerical values are from the 90 K data.

Results and Discussion

The molecular model[18] of oxetane is shown in Figure 2, which also allows a comparison of thermal ellipsoids for the two temperatures. In accordance with the space group symmetry the mirror plane normal to the z axis intersects the molecule at O(1)

---

(15) Stewart, J. M. Technical Report TR-446; University of Maryland: College Park, MD, 1976.

(16) Cromer, D. T.; Mann, J. B. *Acta Crystallogr., Sect. A* **1968**, *A24*, 321.

(17) Stewart, R. F.; Davidson, E. R.; Simpson, W. T. *J. Chem. Phys.* **1965**, *42*, 3175.

(18) Johnson, C. K. ORTEP Report ORNL-3794, 2nd revision; Oak Ridge National Laboratory: Oak Ridge, TN, 1970.

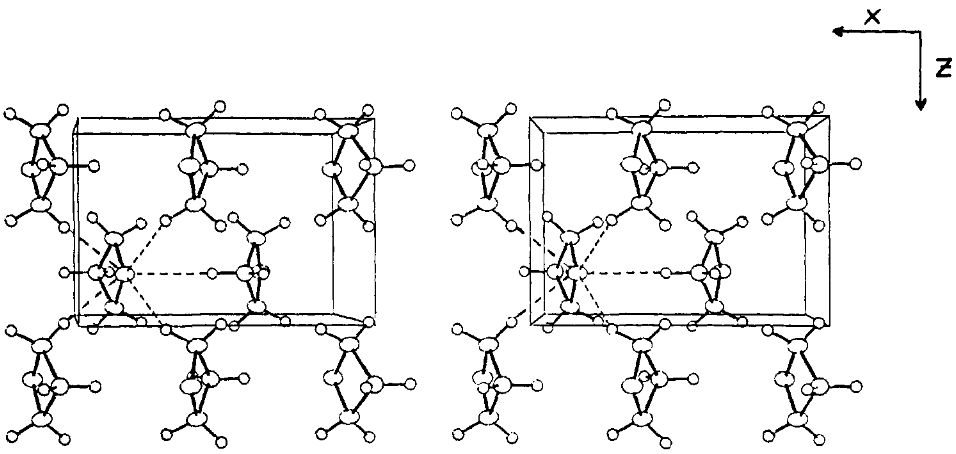

Figure 4. x–z stereoview of the oxetane crystal structure. O- - -H contacts in the range of the van der Waals distance are marked with dashed lines: O(1)- - -H(21) 2.77 (2) Å, symmetry operation for H is $2 - x, -y, {}^1/_2 + z$; O(1)- - -H(21) 2.77 (2) Å ($2 - x, -y, 1 - z$); O(1)- - -H(22) 2.70 (2) Å (${}^3/_2 - x, -{}^1/_2 + y, {}^1/_2 + z$); O(1)- - -H(22) 2.70 (2) Å (${}^3/_2 - x, -{}^1/_2 + y, 1 - z$); O(1)- - -H(31) 2.59 (3) Å ($-{}^1/_2 + x, {}^1/_2 - y, z$).

and C(3) so that the four-membered ring has exact C_s symmetry.

The ring is not planar, and the angle of pucker (that is the dihedral angle of the planes C–O–C and C–C–C) is 10.7 (1)° at 90 K and 8.7 (2)° at 140 K. The deviation from zero is significant. The nonplanarity can also be seen from the ring torsion angles (Table III) which all differ significantly from zero. In all previous investigations with spectroscopic methods or electron diffraction (ED) the oxetane ring was found to be planar or the deviation of the puckering angle from zero was not considered to be significant. This X-ray analysis, however, shows at both temperatures a significant nonplanarity of the ring in the crystal, although the angle of pucker is by far smaller than, for example, the suggested 30° angle in cyclobutane. The single-crystal X-ray investigations on oxetane derivatives[9–11] also showed the ring to be nonplanar, the puckering angle ranging from 4.7° to 22.9° (see Table IV, which gives a survey on previously investigated oxetane derivatives). In view of these and the present results it can be said that the oxetane ring, at least in the crystalline state, is not planar.

The X-ray (XR) bond distances and valence angles we obtained for oxetane are shown in Figure 1, which also gives the atom numbering scheme (C(4) is the mirror image of C(2)). With a comparison of the results from the measurements carried out at the two different temperatures, it is found that the differences in C–H bond distances and valence angles amount to less than three times the statistical error, whereas those in the C–O and C–C distances reach from 8 to 10 times the statistical error, the longer distances belonging to the measurement done at the lower temperature. The U_{eq}'s of the 140 K structure are larger by 40% than those for the 90 K data (see Table II) indicating an appreciably larger thermal motion at the higher temperature (see also Figure 2). This may cause the bond distances to appear shortened. Therefore, the results will be discussed on the basis of the 90 K data.

The XR C–C bond distance was found smaller than that obtained from microwave (MW) data, while the XR C–O bond length (1.460 Å) is even longer than the MW result (1.449 (2) Å). This supports the assumption expressed by Mastryukov[19] that in four-membered rings the C–O bond distance should be unusually large. Also, in the substituted oxetanes (see Table IV) the C–O bonds are longer than C–O single bonds normally are. For comparison, in the five-membered ring of tetrahydrofuran the C–O distance was found to be 1.429 (6) Å (XR)[12] and 1.428 (3) Å[20,21] (ED), and in the dioxane six-membered ring the C–O distance was found to be 1.433 (2) Å[13] (XR at 150 K), and from electron-diffraction data it was 1.423 (3) Å.[22]

The average C–H distance of 0.98 Å represents a normal value for an XR bond of that type. It is considerably smaller than the MW C–H bond length in agreement with the fact that X-ray hydrogen bond lengths are too small.

Considering the three different bond angles in the oxetane ring, the C–C–C and the O–C–C angle agree well with the corresponding MW angles. The angle at the oxygen atom is smaller in the X-ray structure than in the MW investigation. Table IV shows that in all MW or ED investigations the C–O–C angle was found (or set) larger than the O–C–C angle, whereas all X-ray investigations suggest the opposite.

The average hydrogen bond angles are H–C–H at 90 K 110 (1) and at 140 K 110 (2)°; H–C–C at 90 K 116 (2) and at 140 K 116 (2)°; H–C–O at 90 K 110 (1) and at 140 K 111 (1)°. The hydrogen atoms are in almost eclipsed positions, as the puckering of the oxetane ring allows some deviations from an exact eclipsed arrangement (Figure 3). Relative to the ring mean plane[23] the C–H bond vectors have angles between 46° and 60° so that the hydrogen atoms can be regarded as positioned bisectionally.

In the crystal lattice of oxetane (see Figure 4) there are five intermolecular O- - -H contacts close to or less than the van der Waals O- - -H distance of 2.72 Å (van der Waals radii of 1.52 Å for O and 1.20 Å for H are assumed[24]). The smallest O- - -H contact O(1)- - -H(31) is in the crystallographic mirror plane at $z = {}^1/_4, {}^3/_4, \ldots$. Since only one contact of this type is in this plane, the oxygen atom has an asymmetric packing environment in the mirror plane which may have influence on the ring conformation. Other close intermolecular contacts were not observed.

Acknowledgment. The authors are grateful to the Deutsche Forschungsgemeinschaft for making these investigations possible by granting them financial support. They thank, moreover, Eveline Müller for her continuous assistance during this study.

Registry No. Oxetane, 503-30-0.

Supplementary Material Available: Listings of complete atomic parameters with the anisotropic temperature factors for non-hydrogen atoms and isotropic thermal parameters for hydrogen atoms and observed and calculated structure factors for both data sets (at 90 K and 140 K) (10 pages). Ordering information is given on any current masthead page.

---

(19) Mastryukov, V. S.; Osina, E. L.; Vilkov, L. V. *Zh. Strukt. Khim.* **1975**, *16*, 850.
(20) Geise, H. J.; Adams, W. J.; Bartell, L. S. *Tetrahedron* **1969**, *25*, 3045.
(21) Almenningen, A.; Seip, H. M.; Willadsen, T. *Acta Chem. Scand.* **1969**, *23*, 2748.
(22) Davis, M.; Hassel, O. *Acta Chem. Scand.* **1963**, *17*, 1181.
(23) Cremer, D.; Pople, J. A. *J. Am. Chem. Soc.* **1975**, *97*, 1354.
(24) Bondi, A. *J. Phys. Chem.* **1964**, *68*, 441.
(25) Hamilton, W. C. *Acta Crystallogr.* **1959**, *12*, 609.
(26) Gibson, J. S.; Harris, D. O. *J. Chem. Phys.* **1971**, *57*, 2318.
(27) Gibson, J. S.; Harris, D. O. *J. Chem. Phys.* **1970**, *52*, 5234.
(28) Schultz, G.; Bartók, M. *Z. Naturforsch., A* **1979**, *34A*, 1130.
(29) George, C.; Lowrey, A. H.; Karle, J., unpublished results.